Journal of Applied Pharmaceutical Science Vol. 8(10), pp 008-016, October, 2018
Available online at http://www.japsonline.com
DOI: 10.7324/JAPS.2018.81002
ISSN 2231-3354

DOE, formulation, and optimization of Repaglinide nanostructured lipid carriers

Shady A. Swidan[1]*, Zeinab N. Mansour[2], Zeinab A. Mourad[2], Nahla A. Elhesaisy[2], Nada A. Mohamed[2], Mohamed S. Bekheet[2], Mohamed A. Badawy[2], Mai M. Elsemeiri[2], Aya E. Elrefaey[2], Amera M. Hassaneen[2]

[1]Department of Pharmaceutics, Faculty of Pharmacy, The British University in Egypt, El-Sherouk City, Egypt.
[2]Undergraduate student of the 5th year, Faculty of Pharmacy, The British University in Egypt, El-Sherouk City, Egypt.

ARTICLE INFO

Received on: 09/07/2018
Accepted on: 23/08/2018
Available online: 31/10/2018

Key words:
Nanostructured lipid carriers, emulsification–ultrasonification, Repaglinide, optimization, DSC.

ABSTRACT

Nanostructured lipid carriers (NLC) are a recent approach for the delivery of poorly soluble drugs with low oral bioavailability. The oral antidiabetic Repaglinide (RPG) was loaded into NLC using emulsification–ultrasonification technique. A design of experiment was constructed to study the formulation variables. The influence of the liquid lipid to the solid lipid ratio and the concentration of the surfactant on mean particle size, zeta potential, and drug entrapment efficiency was demonstrated. The mean particle size ranged from 182 ± 7.9 nm to 452 ± 66.1 nm. All particles were negatively charged and the zeta potential values ranged from −7.9 ± 0.9 mV to −44.4 ± 6.2 mV. The highest entrapment efficiency was obtained with the minimum solid lipid to liquid lipid ratio and lowest surfactant concentration. All RPG–NLC formulae showed biphasic time-dependent *in vitro* release and the studied factors were optimized and the optimum formula was evaluated for *in vitro* release and crystallinity. The *in vitro* release of the optimized formula fitted to the Higuchi diffusion model. In conclusion, this study showed the potential of NLC as a carrier for controlled release of RPG.

INTRODUCTION

Diabetes mellitus (DM) is an important chronic disease, which may cause severe complications if it is not properly controlled (He *et al*., 2015). Those severe complications include cardiovascular problems, high blood pressure, impaired lipid profile, nephropathy, neuropathy, and retinopathy. This makes this disease the seventh worldwide leading cause of death (Kramer *et al*., 2013). DM has two types and type II DM is the most common type and accounts for more than 90% of the cases (Zhu *et al*., 2013).

Different classes of oral hypoglycemic agents are used for the treatment of type II DM. Repaglinide (RPG), (*S*) (+)-2 ethoxy-4-(2[[3-methyl-1[2-(1-piperidinyl)phenyl]-butyl]amino]-2 oxoethyl) benzoic acid, is a new potent blood glucose lowering agent (Figure 1) (Akhtar *et al*., 2013). It belongs to the class of carbamoyl-methyl benzoic acids. It acts by stimulation of the release of insulin from the pancreatic cells by blocking of ATP-sensitive potassium channels in the plasma membrane (Hu *et al*., 2000). Although RPG has an excellent antidiabetic effect, it suffers from certain problems, which diminish its activity and require frequent administration. RPG has a short half-life (about 1 hour), it suffers from a significant first-pass effect and it has a low oral bioavailability of about 50% (Kassem *et al*., 2017).

In order to increase the patient compliance and enhance its oral bioavailability, different RPG nanoparticles were formulated such as nanoemulsions (Akhtar *et al*., 2016), self-nano emulsifying systems (Kamble *et al*., 2013), nanocrystals (Gadadare *et al*., 2015), and solid lipid nanoparticles (Ebrahimi *et al*., 2015). One of the most promising novel nano-based techniques is nanostructured lipid carriers (NLC). NLC is a new improved generation of solid lipid nanoparticles (SLN), in which a spatially incompatible liquid lipid is added to the solid lipid to form less ordered

*Corresponding Author
Shady A. Swidan, Department of Pharmaceutics, Faculty of Pharmacy, The British University in Egypt, El-Sherouk City, Egypt.
E-mail: shady.swidan @ bue.edu.eg

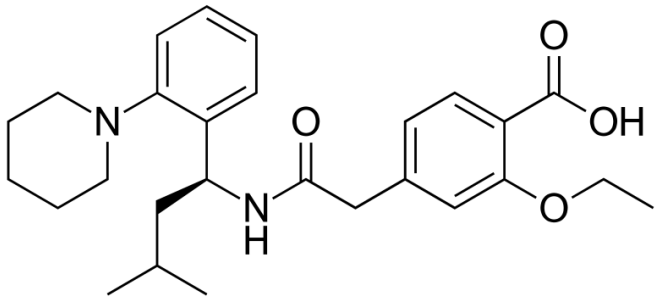

Figure 1. Chemical structure of RPG.

lipid nanoparticles (Swidan *et al*., 2016). It overcomes the disadvantages of SLN, including the low entrapment efficiency and drug loading, especially upon storage due to the drug expulsion from the highly ordered solid lipid crystals. The presence of the liquid lipid disrupts the symmetry of the lipid crystals and shows imperfection of the crystals, thus allowing more drug to be incorporated and lower amount to leave the crystals upon storage while maintaining the solid state at both room and body temperatures (Weber *et al*., 2014).

Several methods can be used for the preparation of NLC such as microemulsion, solvent diffusion, solvent injection, double emulsion, and emulsification ultrasonification (Das and Chaudhury, 2011). In this study, emulsification–ultrasonification method was used as it has a number of advantages; it avoids the use of organic solvents, which may cause toxicity, it is also simple and leads to the formation of small and uniform nanoparticles.

Different factors affect the shape, size, and the function of NLC such as types of solid lipids and liquid lipids, the ratio of both lipids to each other and to the drug, the type and concentration of surfactants, and other different factors related to the preparation technique (Tan *et al*., 2010; Yang *et al*., 2014).

In this study, the objective was to apply response surface methodology optimization model to optimize RPG loaded NLC. Two formulation factors were selected as independent variables. The prepared formulae were characterized by the determination of particle size (PS), polydispersibility index (PDI), and zeta potential (ZP). Entrapment efficiency (EE%), drug loading (DL%), and *in vitro* RPG release were evaluated and the optimized formula was evaluated with the same experiments and the crystallinity of the optimized form was studied using differential scanning calorimetry (DSC). The shape and morphology of the optimized formula were examined using a transmission electron microscope (TEM).

MATERIALS AND METHODS

Materials

RPG and the solid lipid glyceryl monostearate (GMS) are kind gifts from EIPICO pharmaceutical company. Oleic acid (OA) was purchased from Chemajet (Egypt). Polyoxyethylenesorbitan monooleate (Tween 80)—the used surfactant—was purchased from Acros (Netherlands). Potassium dihydrogen phosphate and sodium hydrogen phosphate were purchased from Lobechem (India). All other chemicals and solvents are of pharmaceutical grade and were used with no further modifications.

Methods

Experimental design

Two independent variables were selected for the study, the ratio of the liquid lipid to the solid lipid and the concentration of surfactant. Each factor has three levels: high, medium, and low. The dependent variables or the responses to be determined are the mean PS, ZP and EE%. Values and constraints of both independent variables and responses are listed in Table 1. A 3^2 factorial design was done and the composition of the nine resulted formulae is listed in Table 2. The optimization was done by response surface methodology using Statgraphics® centurion XVII software.

Preparation of RPG loaded (NLCs)

The RPG–NLCs formulae were prepared by emulsification and ultrasonification technique (Das *et al*., 2011) with few modifications. The organic phase—composed of the calculated weights of RPG, the liquid lipid OA, and the solid lipid GMS—was melted by heating up to 5°C above the melting point of GMS. The aqueous phase was prepared by dissolving tween 80 in water and heated to the same temperature as that of molten lipid phase. The preheated aqueous solution was added to the molten lipid phase and homogenized using WiseTis homogenizer HG-15D (Diahan sci, South Korea) for 5 minutes at 10,000 rpm. The coarse hot O/W emulsion obtained was sonicated using a probe sonicator for 1 minute with a pause for 30 seconds for two cycles at 50 W (Vibra cell, Sonics, USA). The obtained NLCs were cooled to room temperature and stored at 4°C.

Table 1. Values of independent and dependent variables.

	Levels		
	Low (%)	**Medium (%)**	**High (%)**
Independent variables			
X_1 Liquid lipid ratio (to the solid lipid)	15	30	45
X_2 Surfactant concentration	1	1.5	2
Dependent variables		Constraints	
Y_1 Particle size		Minimize	
Y_2 Zeta potential		Maximize	
Y_3 Entrapment efficiency		Maximize	

Table 2. Composition of the prepared NLC formulae.

Form.	**RPG (%)**	**Lipids (%)**	**S:L***	**Tween 80 (%)**	**Water (ml)**
F1	0.05	2	85:15	1.5	20
F2	0.05	2	85:15	2	20
F3	0.05	2	70:30	2	20
F4	0.05	2	85:15	1	20
F5	0.05	2	70:30	1	20
F6	0.05	2	70:30	1.5	20
F7	0.05	2	55:45	1	20
F8	0.05	2	55:45	1.5	20
F9	0.05	2	55:45	2	20

*S:L solid lipid to liquid lipid ratio.

Characterization of RPG–NLC

Particle size analysis

The mean PS of the RPG-NLC and the particle size distribution expressed by the PDI of the prepared NLCs were determined using the dynamic light scattering (DLS) technique with Nanotrac particle size analyzer (Microtrac, USA). RPG-NLC samples were diluted by distilled water and the concentration of samples was adjusted for the optimal measurement condition. Three measurements were averaged for the mean PS and PDI and the standard deviation (SD) was calculated.

Zeta potential analysis

The measurement of the electric charge on the surface of the nanoparticles is a good indication of the physical stability of the most colloidal system (Dubey *et al*., 2012). The surface charge of the prepared RPG–NLC was measured by determining ZP on the nanoparticles surface. ZP was measured using Zetatrac W3547 (Microtrac, USA). Conductivity was in the range of 24–42 µs/cm and the applied field strength was 10 kV/m with zeta run time of 30 seconds.

Determination of entrapment efficiency and drug loading of RPG-loaded NLCs

Both EE% and DL% were calculated by measuring the amount of free non-encapsulated RPG in the prepared RPG–NLC. Samples were centrifuged using cooling centrifuge (Centurion Scientific Ltd., UK) as mentioned by Chalikwar *et al*. (2012) with small modifications. Briefly, 1.5 ml of the NLCs dispersion is centrifuged while the speed of centrifuge was kept at 15,000 rpm for 60 min at temperature of 4º C. After suitable dilution, the concentration of RPG in the supernatant was measured using spectrophotometer (Jenway 6305 spectrophotometer, China) at λ_{max} 237 nm. EE% and DL% were calculated using the Equations 1 and 2. The experiment was done in triplicates and the average and SD were calculated.

$$EE\% = \frac{\text{total weight of RPG} - \text{weight of RPG in supernatant}}{\text{total weight of RPG}} \times 100 \quad (1)$$

$$DL\% = \frac{\text{total weight of RPG} - \text{weight of RPG in supernatant}}{\text{total weight of lipid}} \times 100 \quad (2)$$

In vitro release study

The *in vitro* RPG release from the RPG-NLC test was done using dialysis bag diffusion technique (Ebrahimi *et al*., 2015). Dialysis bags used was with a molecular weight cut off 12,000–14,000 were soaked in the release medium for 24 hours before use. Volume equivalent to 1 mg of RPG of RPG suspension and RPG–NLC was added into a thoroughly sealed by double-folding on both sides dialysis bag, which was immersed in 50 ml of simulated intestinal fluid (phosphate buffered saline, PBS, PH 6.8) at 37°C ± 0.5°C. Then, it was placed on shaking water bath at 50 rpm (Wise® bath—water bath, Wised B, Germany) for 24 hours. At predefined time intervals, 1 ml sample was withdrawn from dissolution medium and the amount of RPG released was analyzed spectrophotometrically at λ_{max} 237 nm. The volume of dissolution medium was kept constant by the addition of replacement volumes of PBS after each sampling.

Optimization and preparation of the optimized formula

The relationship between responses and formulation variables of all prepared RPG–NLC were treated using a three-level factorial design model, which is a response surface technique done by the use of Statgraphics® Centurion software. These high, medium and low levels of variables X_1 and X_2 were selected from different preliminary experimentation. The optimization of variables was performed using the desirability function to obtain the levels of X_1 and X_2, which minimize Y_1 while maximizing Y_2 and Y_3.

Characterization of the optimized formula

The optimized prepared formula was characterized by determining PS, PDI, ZP and its morphology and size were studied using TEM technique. Then, the EE% and DL% were also calculated and the *in vitro* release behavior was studied and the best fitted kinetic model for the *in vitro* release was investigated. The crystallinity and polymorphism of the optimized formula were studied using the DSC technique.

TEM

The TEM measurement was done using the negative staining method as reported by Yu and Huang (2013), using electron microscope JTEM-1010, (JEOL®, Tokyo, Japan). One drop of the dispersion of the RPG-NLC was put on a copper grid coating and the excess droplets were wiped using filter paper. After 5 minutes, one drop of uranyl acetate solution (2% w/v) was then dropped onto the grids. After the samples were negatively stained and air-dried at room temperature, they were ready for the TEM investigation done at 74 kV.

Kinetic study of the in vitro drug release of the optimized RPG-NLC formula

The *in vitro* release of the RPG from the optimized formula was evaluated in comparison with the pure RPG. The dissolution medium and the conditions of the experiment were not changed from the conditions mentioned previously for the *in vitro* release of the nine prepared formulae.

RPG release data of the optimized formula were fitted to several mathematical models to know the RPG release mechanism from RPG–NLC in the simulated intestinal fluid. The models studied are zero-order model (percentage cumulative drug released *vs.* time), first-order model (log percentage cumulative drug remained *vs.* time), Higuchi diffusion model (percentage cumulative drug released *vs*. square root of time), and Hixon-Crowell model (cube root of percentage cumulative drug remaining *vs*. time) and the best-fitted model is the model with the highest correlation coefficient (*r*).

Differential scanning calorimetry analysis

DSC analysis was done on the optimized formula, which was lyophilized to study the physical state and polymorphism of the RPG–NLC. The DSC measurements were performed using differential scanning calorimeter, Shimadzu DSC-50 (Japan). The four studied powders were the pure GMS, pure RPG, physical mixture in the ratio (1:1), and the lyophilized optimized RPG–NLC formulae. In brief, samples of weight 2–5 mg were heated, then scanned between 20°C and 250°C. The heating rate was of

10°C minute^{-1} and the measurements were done under nitrogen gas flow (30 ml minute^{-1}) (Mazumder *et al*., 2017).

RESULTS AND DISCUSSION

Particle size analysis

Size of the nanoparticles plays a key role in the evaluation of the efficiency of nanoparticles for RPG delivery. The mean PS and PDI of RPG–NLC is listed in Table 3. The mean PS ranged from 182.7 ± 07.9 in formula F9 to 452.0 ± 66.1 in formula F2, while the narrowest PS distribution was in F7 with PDI of 0.09 ± 0.06, while the widest distribution with PDI of 0.54 ± 0.01 was in F5. The polynomial equation obtained by the linear regression of the data of particle size is shown in Equation 3

$$Y_1 = 365.55 + 6.65611 * X_1 - 282.233 * X_2 + 0.165111 * X_1^2 - 12.21 * X_1 * X_2 + 216.0 * X_2^2 \quad (3)$$

Where Y_1, X_1, and X_2 are the particle size, liquid lipid concentration, and surfactant concentration, respectively.

As seen from the data illustrated in Figure 2A, the smallest PS obtained when the liquid lipid ratio was 45% with the higher concentration of tween 80. This was in agreement with what stated in Kumar *et al*. (2013), who found that the highest percentage of tween 80 surfactant gave the lowest PS. Concerning the percentage of liquid lipid, Teeranachaideekul *et al*. (2008) found that the increase in the amount of liquid lipid should result in an increase in the mean PS of NLCs. Different findings were mentioned by Abdelbary and Haider (2011) who stated that there is no significant effect of liquid lipid to solid lipid ratio on the size of NLC formulae.

Zeta potential

RPG–NLC with high ZP is likely of better stability upon storage than the formulae of ZP value close to 0 mV. It is known that ZP values of more than ±30 are considered a good indication for the stability of the nanoparticles (Honary and Zahir, 2013). As shown in Table 3, Formula F7 showed the highest negative ZP value of −44.4 ± 6.25, while F2 showed the smallest value of −07.9 ± 0.93. The linear regression of the zeta potential data of the prepared formulae resulted in Equation 4

$$Y_2 = -15.9333 + 0.65 * X_1 + 33.4 * X_2 + 0.011037 * X_1^2 - 0.311111 * X_1 * X_2 - 10.6667 * X_2^2 \quad (4)$$

Table 3. Mean PS, PDI, ZP, EE, and DL of RPG–NLC prepared formulae.

Form.	PS (nm)	PDI	ZP (mV)	EE (%)	DL (%)
F1	214.4 ± 33.6	0.25 ± 0.02	−15.4 ± 2.16	81.9 ± 0.95	2.05 ± 0.06
F2	452.0 ± 66.1	0.11 ± 0.03	−07.9 ± 0.93	78.7 ± 1.23	1.97 ± 0.08
F3	281.9 ±12.4	0.17 ± 0.03	−15.9 ± 1.80	74.7 ± 0.82	1.87 ± 0.06
F4	313.0 ± 09.8	0.39 ± 0.03	−40.2 ± 3.22	85.5 ± 0.95	2.14 ± 0.13
F5	195.2 ± 20.8	0.54 ± 0.01	−26.9 ± 3.04	84.2 ± 2.14	2.10 ± 0.08
F6	312.0 ± 37.6	0.12 ± 0.02	−25.6 ± 5.55	80.2 ± 1.66	2.00 ± 0.12
F7	410.0 ± 42.2	0.09 ± 0.06	−44.4 ± 6.25	82.6 ± 2.06	2.06 ± 0.15
F8	229.0 ± 48.2	0.50 ± 0.03	−21.2 ± 5.35	81.0 ± 1.18	2.02 ± 0.12
F9	182.7 ± 07.9	0.35 ± 0.03	−31.8 ± 2.80	78.9 ± 1.98	1.96 ± 0.07

Where Y_2, X_1, and X_2 are the zeta potential, liquid lipid concentration, and surfactant concentration, respectively.

As seen from Figure 2B, no significant effect of Tween 80 concentration on the ZP value was observed. This might be due to the nature of Tween 80 as a non-ionic surfactant. It was noticed that formulae with higher content of OA in the RPG–NLC resulted in an increase in the ZP values and vice versa. This was suggested to be due to the presence of the carboxylic (COO^-) group in the OA. This was in complete agreement with the finding Teeranachaideekul *et al*. (2007) who stated that because of the negative charged medium chain triglycerides at their (COO^-) group, increasing the % of medium chain triglycerides increases the ZP of NLC, and in the absence of the solid lipid, the nano-emulsion showed the highest ZP values.

Entrapment efficiency and drug loading of RPG-loaded NLCs

The percentages of RPG entrapped in all RPG–NLC are listed in Table 3. From table 3 and figure 2C, it is clear that high values of EE% achieved and most of the RPG was entrapped in the nanoparticles. The lowest EE value was 74.7% ± 0.82% in formula 3 with 30% OA and 2% Tween 80, while the highest EE% value was 85.5% ± 0.95% in F4 which contains the lowest concentration of both liquid lipid and surfactant. As there is no change in the total amount of the lipids or the RPG, the ranking of the DL% of the RPG–NLC formulae was the same as in EE%. F4 showed the highest DL% with 2.14% ± 0.13%, while F3 had DL% of 1.87% ± 0.06%. It was found that high EE% and DL% values were obtained with low surfactant concentration. The polynomial equation of the entrapment efficiency is shown in Equation 5

$$Y_3 = 110.927 - 0.850667 * X_1 - 14.82 * X_2 + 0.00557037 * X_1^2 + 0.326222 * X_1 * X_2 - 1.18667 * X_2^2 \quad (5)$$

Where Y_3, X_1, and X_2 are the entrapment efficiency, liquid lipid concentration, and surfactant concentration, respectively.

The highest three formulae in both EE% and DL% were with 1% Tween 80. This may be due to the enhanced solubilization caused by Tween 80 in the aqueous phase. Luo *et al*. (2006) found the same findings and stated that when the amounts of the emulsifiers increased, the EE% decreased due to the solubilization effect of the emulsifiers which enhance the solubility of the drug in the aqueous phase, not in the lipid nanoparticles. Same findings were reported by Venkateswarlu and Manjunath when they used poloxamer 188 as surfactant; as the percentage of poloxamer 188 increased, the EE% was decreased marginally. This thought to be due to increased solubility of the drug used in the aqueous phase as the percentage of poloxamer 188 increased (Venkateswarlu and Manjunath, 2004).

In vitro RPG release from RPG-NLC nanoparticles

The *in vitro* release of RPG from the NLC compared to pure RPG powder was evaluated for 24 hours in simulated intestinal fluid (pH 6.8). The concentrations of RPG were calculated using constructed calibration curve on RPG concentration range 5–50 µg/ml. The curve was linear and obeys the Beer's Lambert law over the whole concentration range, the equation describes the curve is ($y = 0.02x - 0.0125$) and the $r = 0.9996$. The cumulative percentage released of RPG was illustrated in Figure 3. As seen from the graph, the release of RPG from all RPG–NLC formulae

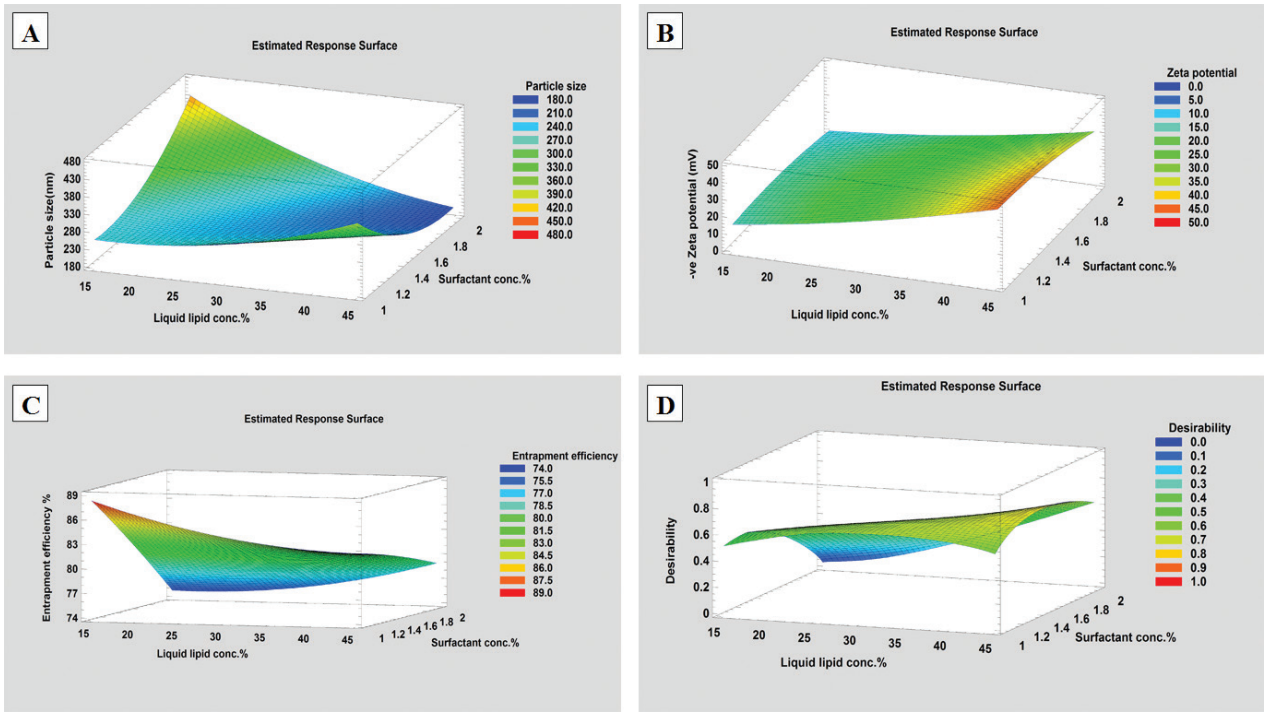

Figure 2. Response surface plots showing the effect of the liquid lipid concentration [*X*1] and surfactant concentration [*X*2] on (A) particle size [*Y*1], (B) zeta potential [*Y*2], (C) entrapment efficiency [*Y*3], and (D) desirability function of the three responses [*Y*1, *Y*2 and *Y*3].

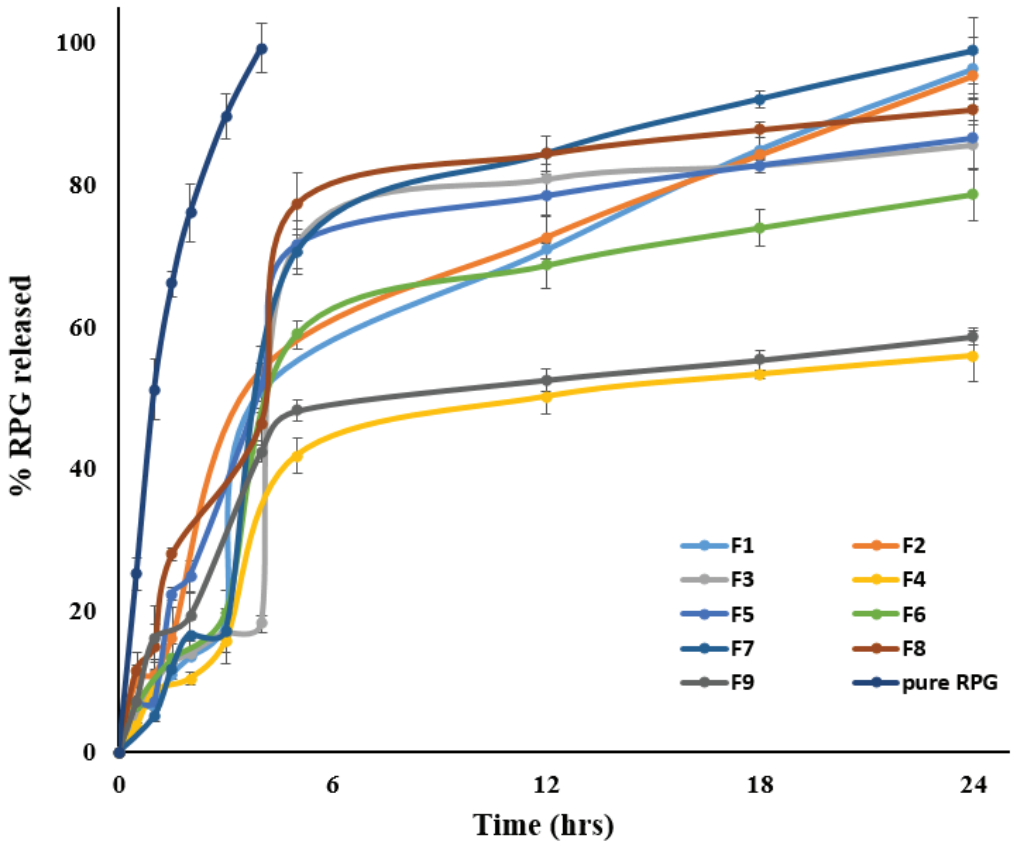

Figure 3. The *in vitro* release of RPG from the prepared RPG-NLC formulae compared to the pure RPG powder in the simulated intestinal fluid dissolution medium.

was biphasic with the initial rapid release and sustained release in the second phase. The faster initial release was derived from the diffusion of RPG located at the surface of the nanoparticle, while the slower later one from that incorporated in the NLC core and released in a prolonged pattern via the erosion or degradation of the matrix (Zeng *et al*., 2012).

It is also clear that all formulae showed the slower release of the drug compared to the pure RPG. After 4 hours, the pure RPG dispersion released about 100%, while all prepared formulae released much smaller amount of RPG within the same period. Formula F3 showed the lowest RPG release with only 18.125% ± 1.15% of RPG, while F2 released the highest percentage of RPG 53.875% ± 3.3%. After 24 hours, the release of RPG from F4 was only 55.90% ± 3.6%, while the fastest RPG release from RPG–NLC formulae was about 98.88% ± 4.7% from formula F7. It is clear that the fastest release obtained in the formula with higher liquid lipid content, while the slowest release was when the OA is only 15%. A possible explanation is that the presence of a high percentage of the lipid in the liquid state led to thermodynamic instability which enhances the release of the drug from the nanoparticles.

Optimization of the independent variables

The optimization of the concentration ratio of the liquid lipid to the solid lipid and the surfactant concentration was done using response surface methodology and through the determination of the desirability function.

This statistical function is considered one of the most important functions to optimize variables statistically. It is a function based on the concept that the quality of a formula that has many features is very unacceptable if one of them is outside of a desirable limit. It aims to adjust the formulation or process variable to values that ensure compliance with the criteria of all of the involved responses and so to provide the optimum value of compromise in the desirable joint response. This can be achieved by converting the multiple responses into a single response, then combining the individual responses into a composite function followed by its optimization (Vera Candioti *et al*., 2014).

All values of the optimized variables, predicted and observed responses are listed in Table 4. The optimum values of variables X_1 and X_2 were 45% and 1.476%, respectively. The predicted responses were 242.5 nm, −41.1 mV, and 81.1% for mean PS, ZP, and EE%, respectively. The measurements done after the formulation of the optimized formula—as observed responses—were 228 nm, −38.2 mV, and 80.2%, respectively. Both ZP and EE% showed a better observed response, while the predicted PS was smaller than that actually measured for the optimized formula, the mean PS and size distribution of the optimized formula is shown in Figure 4. All responses were close to the expected values and were within the statistically accepted deviation range. The desirability function for the optimization process equals 0.751189 (Figure 2D), this value is high enough to ensure acceptable values for the three studied responses.

TEM

The TEM photograph of the optimized RPG–NLC formula is shown in Figure 5 with magnification power 80,000 ×. From the photograph, it is clear that the NLC vesicles are separate entities. All particles appeared in the photograph were in the nanometer range. The TEM investigation also revealed that the nanoparticles of the RPG–NLC formula were homogeneous ellipsoidal or spherical in shape. This might indicate homogeneity and good uniformity of the release of the entrapped RPG. It was noticed that the vesicles look smaller in size when measured using TEM technique compared to that measured by DLS technique. As the preparation of the TEM sample involves drying, this leads to shrinkage of the nanoparticles so they appear smaller compared with the DLS measurement, in which the hydration of samples maintains the size of the nanoparticles (Sanad *et al*., 2010).

Table 4. The predicted and the observed response for the optimized RPG-NLC formula.

Independent variables	Optimum value (%)	
X_1 Liquid lipid ratio	45.0	
X_2 Surfactant concentration	1.476	
Dependent variables	Predicted response	Observed response
Y_1 Particle size	242.5 nm	228 nm
Y_2 Zeta potential	−41.1 mV	−38.2 mV
Y_3 Entrapment efficiency	81.1%	80.2%

Kinetic study of the in vitro drug release of the optimized RPG-NLC formula

The *in vitro* release data of the optimized formula showed slower RPG release than all previously prepared NLC formulae. Optimized formula released only 17.13% ± 0.53% of RPG after 4 hours, while after 24 hours, 44.38% ± 2.1% of RPG released. This pattern of release proved that the optimized formulae achieved the controlled prolonged release pattern that allows sustained RPG release, hence better control of DM can be obtained.

Different kinetic models were applied to the RPG release data. RPG release from the optimized formula at pH 6.8 did not show proper fitting to zero order, first order, and Hixon Crowell models and the *r* values were 0.967, −0.979, and 0.976, respectively. The best-fitted model to describe the kinetics of the release and hence describe the release mechanism was Higuchi diffusion model with the highest *r* value equals 0.992. Graphical representation of the application of Higuchi diffusion model to the release data is shown in Figure 6. The fitting of this model suggests that the major mechanism of the RPG release was by diffusion as this model best applied to systems shows release by diffusion through the lipid matrix (Siepmann and Peppas, 2011). This was in complete agreement with the findings of Sangsen *et al*. (2014), which prepared curcumin loaded NLC.

Differential scanning calorimetry analysis

DSC is an accurate, rapid, and reliable method for the characterization of crystallinity of the drug. It also gives a strong indication on the possible interactions that might occur between the drug and all additives, which is reflected in the thermogram by the appearance of new peaks, displacement of the endothermic peaks, or change in their shape or enthalpy (Maiti *et al*., 2007).

The thermograms of pure RPG, pure GMS, physical mixture of both, and the RPG-NLC optimized formula are shown in Figure 7. As seen from the figure, RPG showed a sharp

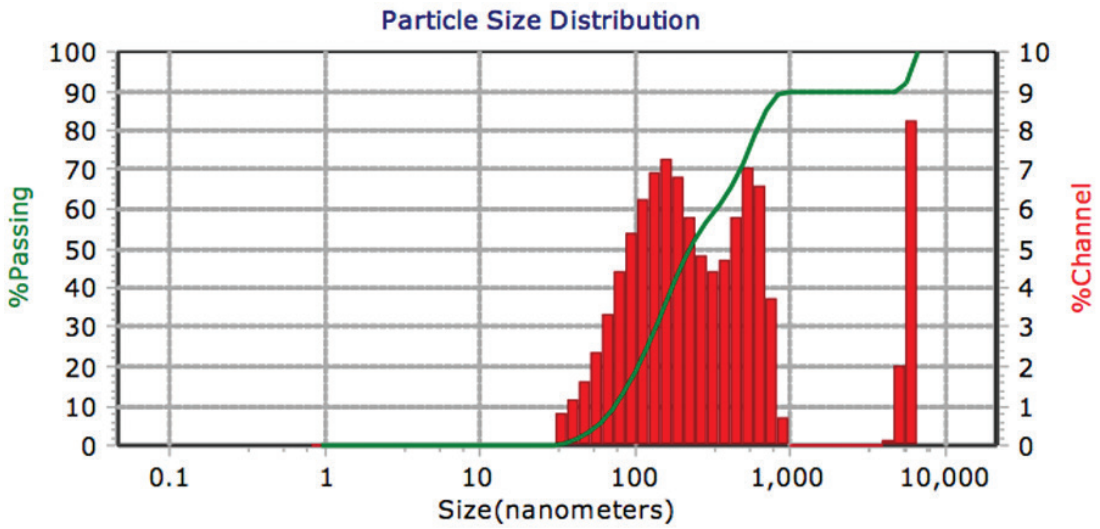

Figure 4. Particle size distribution of the optimized RPG-NLC formula.

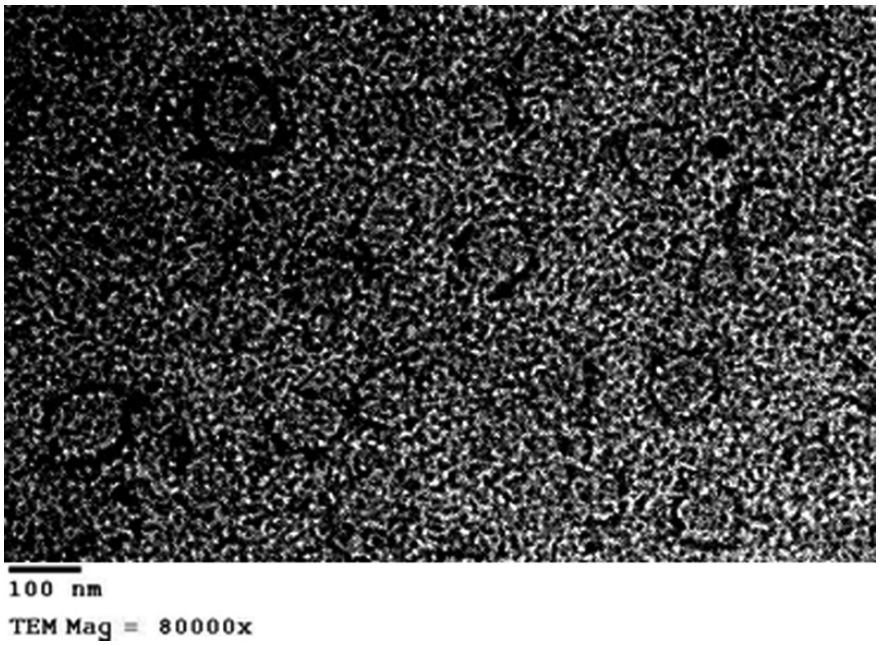

Figure 5. TEM photography of the lyophilized optimized RPG-NLC nanoparticles.

endothermic peak at 131.3°C. This indicates that pure RPG is in the crystalline state and this value was in agreement with Purvis *et al*. (2007).

The GMS showed a sharp single endothermic peak at 69.1°C. The physical mixture of the drug and the lipid showed two endothermic peaks at approximately the same temperatures for the pure powders. A slight widening in the peak of the RPG was noticed which might be an indication of the presence of slight affinity between RPG and GMS, but both are still in the crystalline state and no interaction was noticed. Complete disappearance of the melting peak of the RPG in its melting temperature range was noticed, while a slightly displaced peak for GMS appeared. This finding suggests the conversion of the crystalline RPG to its amorphous state. This signifies the possibility of interaction between the drug and the lipid and indicates a better solubility of the RPG which affects its release from the nanoparticles (Kassem *et al*., 2017).

CONCLUSION

In the current study, the RPG–NLC formulae were successfully prepared using emulsification–ultrasonification method. High RPG entrapment was achieved in the prepared nanosized vesicles. The liquid lipid and surfactant concentrations are crucial for optimizing size, charge, drug loading, drug entrapment, and RPG release from RPG–NLC. RPG–NLC achieved sustained controlled biphasic release *in vitro*, while the release kinetics of the optimized formula obeyed Higuchi diffusion kinetics model. RPG was in an amorphous state in the NLC, which allows better solubility and

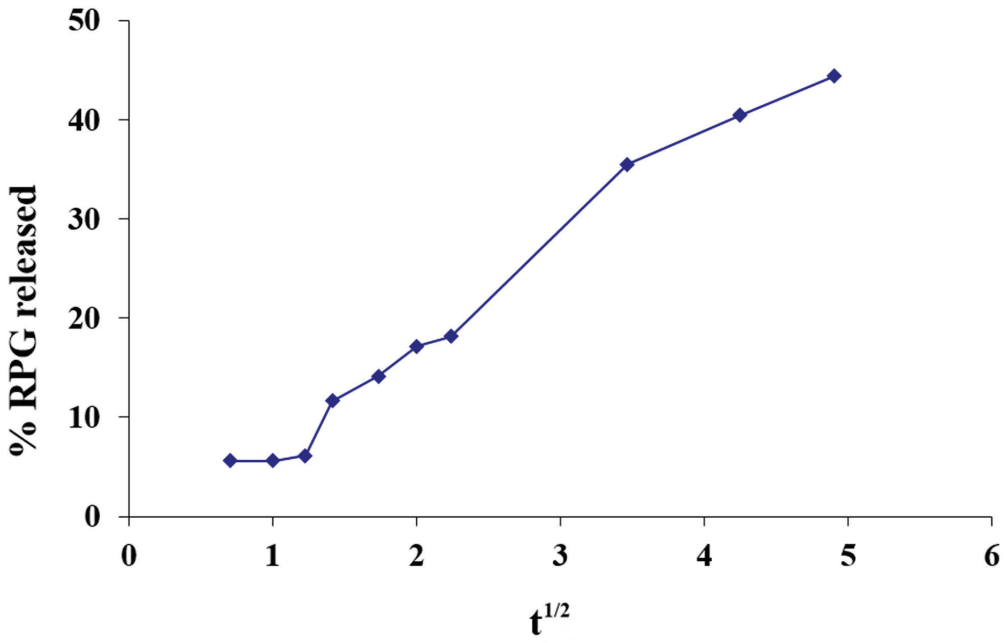

Figure 6. Higuchi diffusion model representation for the *in vitro* release of RPG from the optimized RPG-NLC formula.

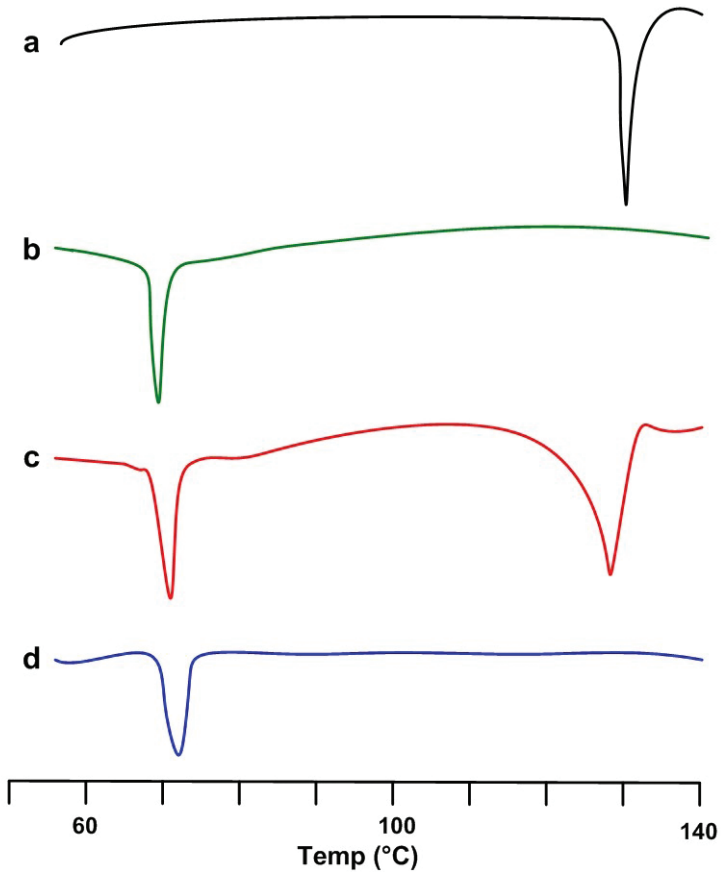

Figure 7. DSC thermograms of (A) pure RPG, (B) pure GMS, (C) physical mixture of RPG and GMS, and (D) optimized RPG-NLC formula.

controlled release. Further studies on the *in vivo* pharmacodynamics, pharmacokinetic, and therapeutic effects must be done. Finally, NLC is a promising nanocarrier for the delivery of RPG orally.

REFERENCES

Abdelbary G, Haider G. In vitro characterization and growth inhibition effect of nanostructured lipid carriers for controlled delivery of methotrexate. Pharm Dev Technol, 2011; 18(5):1159–68.

Akhtar J, Fareed S, Aqil M. Stability-indicating assay of repaglinide in bulk and optimized nanoemulsion by validated high performance thin layer chromatography technique. J Pharm Bioallied Sci, 2013; 5(3):184.

Akhtar J, Siddiqui HH, Fareed S, Badruddeen MK, Aqil M. Nanoemulsion: for improved oral delivery of repaglinide. Drug Deliv, 2016; 23(6):2026–34.

Chalikwar SS, Belgamwar VS, Talele VR, Surana SJ, Patil MU. Formulation and evaluation of nimodipine-loaded solid lipid nanoparticles delivered via lymphatic transport system. Colloids Surf B Biointerfaces, 2012; 97:109–16.

Das S, Chaudhury A. Recent advances in lipid nanoparticle formulations with solid matrix for oral drug delivery. AAPS PharmSciTech, 2011; 12(1):62–76.

Das S, Ng WK, Kanaujia P, Kim S, Tan RBH. Formulation design, preparation and physicochemical characterizations of solid lipid nanoparticles containing a hydrophobic drug: effects of process variables. Colloids Surf B Biointerfaces, 2011; 88(1):483–89.

Dubey A, Prabhu P, Kamath JV. Nano structured lipid carriers: a novel topical drug delivery system. Int J PharmTech Res, 2011; 4(2):705–14.

Ebrahimi HA, Javadzadeh Y, Hamidi M, Jalali MB. Repaglinide-loaded solid lipid nanoparticles: effect of using different surfactants/ stabilizers on physicochemical properties of nanoparticles. Daru, 2015; 23(1):46.

Gadadare R, Mandpe L, Pokharkar V. Ultra rapidly dissolving Repaglinide nanosized crystals prepared via bottom-up and top-down approach: influence of food on pharmacokinetics behavior. AAPS PharmSciTech, 2015; 16(4):787–99.

He W, Wu M, Huang S, Yin L. Matrix tablets for sustained release of Repaglinide: preparation, pharmacokinetics and hypoglycemic activity in Beagle dogs. Int J Pharm 2015; 478(1):297–307.

Honary S, Zahir F. Effect of zeta potential on the properties of nano-drug delivery systems—a review (Part 1). Trop J Pharm Res 2013; 12(2):255–64.

Hu S, Wang S, Fanelli B, Bell PA, Dunning BE, Geisse S, *et al*. Pancreatic beta-cell K (ATP) channel activity and membrane-binding studies with nateglinide: a comparison with sulfonylureas and Repaglinide. J Pharmacol Exp Ther, 2000; 293(2):444–52.

Kamble MS, Borwandkar VG, Bodade SS, Aute PP, Chaudhari PD, Bhosale AV. Optimization of self-nanoemulsifying drug delivery system (SNEDDS) of Repaglinide using D-optimal mixture experimental design. J Biomed Pharm Res, 2013; 2(3):100–8, 109.

Kassem, AA, Abd El-Alim SH, Basha M, Salama A. Phospholipid complex enriched micelles: a novel drug delivery approach for promoting the antidiabetic effect of Repaglinide. Eur J Pharm Sci, 2017; 99:75–84.

Kramer CK, Zinman B, Gross JL, Canani LH, Rodrigues TC, Azevedo MJ, *et al*. Coronary artery calcium score prediction of all cause mortality and cardiovascular events in people with type 2 diabetes: systematic review and meta-analysis. BMJ, 2013; 346(1):1654–4.

Kumar GSS, Talsania MP, Goli D, Karki R. Formulation and optimization of nanostructured lipid matrices of Repaglinide using factorial design. World J Pharm Pharm Sci, 2013; 2(6):5521–37.

Luo YF, Chen DW, Ren LX, Zhao XL, Qin J. Solid lipid nanoparticles for enhancing vinpocetine's oral bioavailability. J Control Release, 2006; 114(1):53–9.

Maiti K, Mukherjee K, Gantait A, Saha BP, Mukherjee PK. Curcumin-phospholipid complex: preparation, therapeutic evaluation and pharmacokinetic study in rats. Int J Pharm, 2007; 330(1–2):155–63.

Mazumder S, Dewangan AK, Pavurala N. Enhanced dissolution of poorly soluble antiviral drugs from nanoparticles of cellulose acetate based solid dispersion matrices. Asian J Phar Sci, 2017; 12(6):532–41.

Purvis T, Mattucci ME, Crisp MT, Johnston KP, Williams RO. Rapidly dissolving Repaglinide powders produced by the ultra-rapid freezing process. AAPS PharmSciTech, 2017; 8(3):E58.

Sanad RA, Abdelmalak NS, Elbayoomy TS, Badawi AA. Formulation of a novel oxybenzone-loaded nanostructured lipid carriers (NLCs). AAPS PharmSciTech, 2010; 11(4):1684–94.

Sangsen Y, Laochai P, Chotsathidchai P, Wiwattanapatapee R. Effect of solid lipid and liquid oil ratios on properties of nanostructured lipid carriers for oral curcumin delivery. Adv Mat Res, 2014; 1060:62–5.

Siepmann J, Peppas NA. Higuchi equation: derivation, applications, use and misuse. Int J Pharm, 2011; 418(1):6–12.

Swidan SA, Ghonaim HM, Samy AM, Ghorab MM. Efficacy and in vitro cytotoxicity of nanostructured lipid carriers for paclitaxel delivery. J Appl Pharm Sci, 2016; 6(9):018–26.

Tan SW, Billa N, Roberts CR, Burley JC. Surfactant effects on the physical characteristics of amphotericin B-containing nanostructured lipid carriers. Colloids Surf A Physicochem Eng Aspects, 2010; 372(1–3):73–9.

Teeranachaideekul V, Boonme P, Souto EB, Müller RH, Junyaprasert VB. Influence of oil content on physicochemical properties and skin distribution of nile red-loaded NLC. J Control Release, 2008; 128(2):134–41.

Teeranachaideekul V, Souto EB, Junyaprasert VB, Müller RH. Cetyl palmitate-based NLC for topical delivery of coenzyme Q10—development, physicochemical characterization and in vitro release studies. Eur J Pharm Biopharm, 2007; 67(1):141–8.

Venkateswarlu V, Manjunath K. Preparation, characterization and in vitro release kinetics of clozapine solid lipid nanoparticles. J Control Release, 2004; 95(3):627–38.

Vera Candioti L, De Zan MM, Cámara MS, Goicoechea HC. Experimental design and multiple response optimization. Using the desirability function in analytical methods development. Talanta, 2014; 124:123–38.

Weber S, Zimmer A, Pardeike J. Solid lipid nanoparticles (SLN) and nanostructured lipid carriers (NLC) for pulmonary application: a review of the state of the art. Eur J Pharm Biopharm, 2014; 86(1):7–22.

Yang Y, Corona A, Schubert B, Reeder R, Henson MA. The effect of oil type on the aggregation stability of nanostructured lipid carriers. J Colloid Interface Sci, 2014; 418:261–72.

Yu H, Huang Q. Bioavailability and delivery of nutraceuticals and functional foods using nanotechnology. Bio-Nanotechnol Revol Food Biomed Health Sci, 2013; 593–604.

Zeng N, Hu Q, Liu Z, Gao X, Hu R, Song Q, *et al*. Preparation and characterization of paclitaxel-loaded DSPE-PEG-liquid crystalline nanoparticles (LCNPs) for improved bioavailability. Int J Pharm, 2012; 424(1–2):58–66.

Zhu H, Zhang X, Li M-Z, Xie J, Yang X-L. Prevalence of type 2 diabetes and pre-diabetes among overweight or obese children in Tianjin, China. Diab Med J Br Diab Assoc, 2013; 30(12):1457–65.

How to cite this article:
Swidan SA, Mansour ZN, Mourad ZA, Elhesaisy NA, Mohamed NA, Bekheet MS, *et al*. DOE, formulation, and optimization of Repaglinide nanostructured lipid carriers. J App Pharm Sci, 2018; 8(10): 008-016.